

A simple model for ultradiscrete Hopf bifurcation

Shousuke Ohmori^{*)} and Yoshihiro Yamazaki

Department of Physics, Waseda University, Shinjuku, Tokyo 169-8555, Japan

**corresponding author: 42261timemachine@ruri.waseda.jp*

Abstract

Dynamical properties of ultradiscrete Hopf bifurcation, similar to those of the standard Hopf bifurcation, are discussed by proposing a simple model of ultradiscrete equations with max-plus algebra. In ultradiscrete Hopf bifurcation, limit cycles emerge depending on the value of a bifurcation parameter in the model. The limit cycles are composed of a finite number of discrete states. Furthermore, the model exhibits excitability. The model is derived from two different dynamical models with Hopf bifurcation by means of ultradiscretization; it is a candidate for a normal form for ultradiscrete Hopf bifurcation.

For analysis of dynamical properties of nonlinear equations, piecewise linearization of them has often been carried out. Especially, ultradiscretization, one of piecewise linearization methods, successfully retains and elucidates the essence of dynamical structures in nonlinear integrable systems [1, 2]. The ultradiscretization method is summarized as follows. Difference equations are derived from given continuous nonlinear equations. By some limiting procedure, the difference equations are converted into other type of difference equations with max-plus algebra, which is called ultradiscrete equation. This limiting procedure produces piecewise linearization of the original equations. Note that the ultradiscretization can be applied to an-

other type of dynamical systems such as non-integrable non-equilibrium dissipative systems and reaction-diffusion systems [3, 4, 5, 6, 7, 8, 9, 10].

Recently, we have applied ultradiscretization to bifurcation phenomena in one-dimensional dynamical systems[10]. Bifurcation phenomena have been hugely studied from viewpoint of continuous[11, 12, 13] and discrete[14, 15, 16] dynamical systems. In our study, focusing on the one-dimensional normal forms of saddle-node, transcritical, and pitchfork bifurcations, their ultradiscrete equations were derived and the dynamical properties for the obtained ultradiscrete equations were investigated. In particular, we found that they possess “ultradiscrete bifurcations”, which has similar properties to the original bifurcations. These ultradiscrete bifurcations can be visually understood by piecewise linear graphs of the ultradiscrete equations.

In this letter, we focus on Hopf bifurcation in two-dimensional dynamical systems. First, we propose a model of ultradiscrete equations which exhibits a bifurcation similar to Hopf bifurcation. Actually, our proposed model shows a dynamical transition between a monostable state and a state with limit cycles. Next, we show that our model can be a normal form of ultradiscrete Hopf bifurcation by deriving it from two different nonlinear dynamical models.

Let us focus on the following model consisting of max-plus equations with a bifurcation parameter B :

$$X_{n+1} = Y_n + \max(0, 2X_n), \quad (1)$$

$$Y_{n+1} = B - \max(0, 2X_n). \quad (2)$$

Eqs. (1)-(2) are considered as a discrete dynamical system $\mathbf{x}_{n+1} = \mathbf{F}(\mathbf{x}_n)$ for the state variable $\mathbf{x}_n = (X_n, Y_n)$, equipping the evolution operator

$$\mathbf{F} : R^2 \rightarrow R^2, (x, y) \mapsto (y + \max(0, 2x), B - \max(0, 2x)). \quad (3)$$

A trajectory $\{\mathbf{x}_0, \mathbf{x}_1, \mathbf{x}_2, \dots\} (\equiv \{\mathbf{x}_n\})$ from the initial point $\mathbf{x}_0 = (X_0, Y_0)$ is given by $\mathbf{x}_n =$

$\underbrace{\mathbf{F} \circ \dots \circ \mathbf{F}}_n(\mathbf{x}_0) = \mathbf{F}^n(\mathbf{x}_0) (n = 1, 2, \dots)$. Here we set the following two regions I and II in (X_n, Y_n) plane as shown in Fig.1 (a): (I) $X_n > 0$ and (II) $X_n \leq 0$. In each region, Eqs. (1)-(2) can be represented as the following matrix form.

(Region I) When $X_n > 0$, Eqs. (1)-(2) can be rewritten as

$$\begin{pmatrix} X_{n+1} \\ Y_{n+1} \end{pmatrix} = \begin{pmatrix} 2 & 1 \\ -2 & 0 \end{pmatrix} \begin{pmatrix} X_n \\ Y_n \end{pmatrix} + \begin{pmatrix} 0 \\ B \end{pmatrix}, \quad (4)$$

where Eq. (4) has the fixed point $\bar{\mathbf{x}}_I = (B, -B)$. The matrix $\mathbf{A}_I = \begin{pmatrix} 2 & 1 \\ -2 & 0 \end{pmatrix}$ satisfies $\text{Tr}\mathbf{A}_I = \det\mathbf{A}_I = 2$, where Tr and \det stand for trace and determinant of a matrix, respectively. Therefore, the trajectory given by Eq. (4) is characterized as a clockwise spiral source[16], whose center is the unstable fixed point $\bar{\mathbf{x}}_I$. Fig. 1(b) shows the trajectory of $\{\mathbf{x}_n\}$ with $\mathbf{x}_0 = (1, 0)$ and $B = 0$.

(Region II) When $X_n \leq 0$, the matrix form of Eqs. (1)-(2) is

$$\begin{pmatrix} X_{n+1} \\ Y_{n+1} \end{pmatrix} = \begin{pmatrix} 0 & 1 \\ 0 & 0 \end{pmatrix} \begin{pmatrix} X_n \\ Y_n \end{pmatrix} + \begin{pmatrix} 0 \\ B \end{pmatrix}. \quad (5)$$

Equation (5) has the fixed point $\bar{\mathbf{x}}_{II} = (B, B)$. For the matrix $\mathbf{A}_{II} = \begin{pmatrix} 0 & 1 \\ 0 & 0 \end{pmatrix}$, $\text{Tr}\mathbf{A}_{II} = \det\mathbf{A}_{II} = 0$. The fixed point $\bar{\mathbf{x}}_{II}$ becomes a stable node. Actually for any $\mathbf{x}_0 = (X_0, Y_0)$, it is readily found that $\mathbf{x}_1 = (Y_0, B)$ and $\mathbf{x}_2 = (B, B) = \bar{\mathbf{x}}_{II}$; Fig. 1 (c) shows an example.

Taking these dynamical properties in regions I and II into account, bifurcation for Eqs. (1)-(2), can be grasped as follows. (i) When $B \leq 0$, both $\bar{\mathbf{x}}_I$ and $\bar{\mathbf{x}}_{II}$ are in region II; $\bar{\mathbf{x}}_{II}$ becomes a fixed point, but $\bar{\mathbf{x}}_I$ does not. Then, Eqs. (1)-(2) have a unique fixed point $\bar{\mathbf{x}}_{II} = (B, B)$. (i-a) When $\mathbf{x}_0 = (X_0, Y_0)$ belongs to “region II-1”, which means $X_0 \leq 0$ and $Y_0 \leq 0$, $\mathbf{x}_1 = (Y_0, B)$ and $\mathbf{x}_2 = (B, B) = \bar{\mathbf{x}}_{II}$. Then any initial point in region II-1 reaches $\bar{\mathbf{x}}_{II}$ with two iteration steps. (i-b) \mathbf{x}_0 in region I moves into region II-1 within four iteration steps as shown in Fig.2. Then, any initial point in region II-1 reaches $\bar{\mathbf{x}}_{II}$ within six steps. (i-c) When \mathbf{x}_0 is in “region

II-2", which shows $X_0 \leq 0$ and $Y_0 > 0$, $\mathbf{x}_1 = (Y_0, B)$ belongs to region I. Therefore, \mathbf{x}_0 reaches $\bar{\mathbf{x}}_{II}$ within seven steps from the property (i-b). From (i-a)-(i-c), it is found that the fixed point $\bar{\mathbf{x}}_{II} = (B, B)$ is stable. The trajectories of $\{\mathbf{x}_n\}$ in this case are shown in Fig. 3. Figure 3 also shows that excitability occurs when \mathbf{x}_0 is in region II-2. Figure 4 shows time evolutions of (X_n, Y_n) from two different initial conditions. By comparing with Fig.4(a), it is found that excitability occurs in Fig.4(b). (ii) When $B > 0$, $\bar{\mathbf{x}}_I = (B, -B)$ becomes a unique unstable fixed point. We find that there exist only two different clockwise periodic solutions, \mathcal{C} and \mathcal{C}_s as shown in Fig.5(a), which are composed of the following seven points, respectively: $\mathcal{C} = \{(B, B) \rightarrow (3B, -B) \rightarrow (5B, -5B) \rightarrow (5B, -9B) \rightarrow (B, -9B) \rightarrow (-7B, -B) \rightarrow (-B, B) [\rightarrow (B, B)]\}$, $\mathcal{C}_s = \{(\frac{B}{15}, B) \rightarrow (\frac{17B}{15}, \frac{13B}{15}) \rightarrow (\frac{47B}{15}, -\frac{19B}{15}) \rightarrow (5B, -\frac{79B}{15}) \rightarrow (\frac{71B}{15}, -9B) \rightarrow (\frac{7B}{15}, -\frac{127B}{15}) \rightarrow (-\frac{113B}{15}, \frac{1B}{15}) [\rightarrow (\frac{B}{15}, B)]\}$. It is also found that a trajectory with any initial condition except for $\bar{\mathbf{x}}_I$ is finally absorbed in \mathcal{C} or \mathcal{C}_s . Therefore, \mathcal{C} and \mathcal{C}_s are considered as limit cycles. Figure 5(b) shows trajectories from four different initial conditions; they finally converge into \mathcal{C} .

Here we discuss basins for \mathcal{C} and \mathcal{C}_s . It is confirmed that any trajectory has a point with $Y_n = B$ at a certain iteration step n . In other words, a point on the line l_B , $\mathbf{x}_n = (X_n, B)$ where $X_n \in (-\infty, \infty)$, exists in all trajectories. It is found that all trajectories with a point on l_B except for $(\frac{B}{15}, B)$ and $(\frac{17B}{15}, B)$ are finally absorbed into \mathcal{C} . And any trajectory with $(\frac{B}{15}, B)$ or $(\frac{17B}{15}, B)$ finally goes into \mathcal{C}_s . Therefore, there exist only two limit cycles \mathcal{C} and \mathcal{C}_s in this model.

Now we show that Eqs. (1)-(2) become a candidate of a normal form of ultradiscrete Hopf bifurcation. Through ultradiscretization, Eqs. (1)-(2) can be derived from the following two different dynamical systems described by partial differential equations.

(i) Sel'kov model[12, 17]

$$\frac{dx}{dt} = -x + ay + x^2y, \quad (6)$$

$$\frac{dy}{dt} = b - ay - x^2y, \quad (7)$$

where a and b are positive. They can be considered as bifurcation parameters for Hopf bifurcation. Actually, eqs. (6)-(7) exhibit Hopf bifurcation when a and b satisfy $b^2 = \frac{1}{2}(1-2a \pm \sqrt{1-8a})$.

Ultradiscretization of Sel'kov model can be performed in the following way. By tropical discretization[4], the following difference equations are adopted for eqs. (6)-(7),

$$x_{n+1} = \frac{x_n + \Delta t(ay_n + x_n^2y_n)}{1 + \Delta t}, \quad (8)$$

$$y_{n+1} = \frac{y_n + \Delta tb}{1 + \Delta t(a + x_n^2)}, \quad (9)$$

where Δt is the discretized time interval. $x_n = x(n\Delta t)$, $y_n = y(n\Delta t)$, where n is positive integer.

The variable transformations,

$$\begin{cases} \Delta t = e^{T/\varepsilon}, & x_n = e^{X_n/\varepsilon}, & y_n = e^{Y_n/\varepsilon}, \\ a = e^{A/\varepsilon}, & b = e^{B/\varepsilon}, \end{cases} \quad (10)$$

are applied to eqs.(8)-(9), and the ultradiscrete limits

$$\begin{cases} \lim_{\varepsilon \rightarrow +0} \varepsilon \log(e^{A/\varepsilon} + e^{B/\varepsilon} + \dots) = \max(A, B, \dots), \\ \lim_{\varepsilon \rightarrow +0} \varepsilon \log(e^{A/\varepsilon} \cdot e^{B/\varepsilon} \cdot \dots) = A + B + \dots \end{cases} \quad (11)$$

are performed. Then, the ultradiscrete equations for Sel'kov model are obtained as

$$X_{n+1} = \max(X_n, T + \max(A + Y_n, 2X_n + Y_n)) - \max(0, T), \quad (12)$$

$$Y_{n+1} = \max(Y_n, T + B) - \max(0, T + \max(A, 2X_n)). \quad (13)$$

Assuming that $T \geq \max\{0, -A, Y_n - B, -(X_n + Y_n)\}$ for all n and $A = 0$, eqs. (12)-(13) are identical to eqs.(1)-(2).

(ii) Lengyel model [18, 19],

$$\frac{dx}{dt} = r - x - \frac{4xy}{1+x^2}, \quad (14)$$

$$\frac{dy}{dt} = x(1 - \frac{sy}{1+x^2}), \quad (15)$$

where r and s are positive bifurcation parameters for Hopf bifurcation. Ultradiscrete equations of Eqs. (14)-(15) are obtained in the similar way to the case of Eqs. (6)-(7). By tropical discretization, the following difference equations are derived from Eqs. (14)-(15),

$$x_{n+1} = \frac{x_n + \Delta t(r - x_n)}{1 + \Delta t(\frac{4y_n}{1+x_n^2})}, \quad (16)$$

$$y_{n+1} = \frac{y_n + \Delta t x_n}{1 + \Delta t(\frac{s x_n}{1+x_n^2})}. \quad (17)$$

The variable transformations,

$$\begin{cases} \Delta t = e^{T/\varepsilon}, & 1 - \Delta t = e^{M/\varepsilon}, & x_n = e^{X_n/\varepsilon}, & y_n = e^{Y_n/\varepsilon}, \\ r = e^{R/\varepsilon}, & s = e^{S/\varepsilon}, \end{cases} \quad (18)$$

and ultradiscrete limits (11) are carried out. Then, the ultradiscrete equations for Lengyel model are obtained as

$$X_{n+1} = R - Y_n + \max(0, 2X_n), \quad (19)$$

$$Y_{n+1} = -S + \max(0, 2X_n), \quad (20)$$

on the assumption $T \geq \max\{0, X_n + M - R, Y_n - X_n, |X_n| - S\}$ for all n . It is noted that Eqs.(19)-(20) have counterclockwise limit cycles reflected on the signs in the equations. Therefore taking the variable transformations $Y_n \rightarrow -Y_n$ and setting $R = 0, S = B$ in Eqs.(19)-(20), Eqs.(1)-(2) can be reproduced.

In conclusion, we have proposed the simple model for ultradiscrete Hopf bifurcation. Depending on the value of the bifurcation parameter, the model exhibits excitability and possesses the limit cycles. The model is derived from the two different nonlinear dynamical models, Sel'kov

model and Lengyel model; it can be a normal form of ultradiscrete Hopf bifurcation. Further investigation for basins of \mathcal{C} and \mathcal{C}_s and characterization for their periodicity will be future problems.

Acknowledgement

The authors are grateful to Prof. M. Murata, at Tokyo University of Agriculture and Technology, Prof. K. Matsuya at Musashino University, Prof. D. Takahashi, Prof. T. Yamamoto, and Prof. Emeritus A. Kitada at Waseda University for useful comments and encouragements. This work was supported by Sumitomo Foundation, Grant Number 200146.

References

- [1] T. Tokihiro, D. Takahashi, J. Matsukidaira, and J. Satsuma, Phys. Rev. Lett. **76**, 3247 (1996).
- [2] B. Grammaticos, Y. Ohta, A. Ramani, D. Takahashi, and K. M. Tamizhmani, Phys. Lett. A **226**, 53 (1997).
- [3] T. Nagatani, Phys. Rev. E **58** 700 (1998).
- [4] M. Murata, J. Differ. Equations Appl. **19** 1008 (2013).
- [5] S. Ohmori and Y. Yamazaki, Prog. Theor. Exp. Phys. 08A01 (2014).
- [6] K. Matsuya and M. Murata, Discrete Contin. Dyn. Syst. B **20** 173 (2015).
- [7] M. Murata, J. Phys. A Math, Theor. **48** 255202 (2015).
- [8] S. Gibo and H. Ito, J. Theor. Biol. **378** 89 (2015).
- [9] S. Ohmori and Y. Yamazaki, J. Phys. Soc. Jpn. **85** 045001 (2016).

- [10] S. Ohmori and Y. Yamazaki, J. Math. Phys. **61** 122702 (2020)
- [11] J. Guckenheimer and P. Holmes, *Nonlinear Oscillations, Dynamical Systems, and Bifurcations of Vector Fields* (Springer, New York, 1983).
- [12] Steven. H. Strogatz, *Nonlinear Dynamics and Chaos* (Westview Press, U.S. 1994).
- [13] G. Nicolis, *Introduction to Nonlinear Science* (Cambridge Univ. Press 1995).
- [14] C. Robinson, *Dynamical systems -Stability, Symbolic Dynamics, and Chaos-, 2ed edition* (CRC Press, Florida 1999).
- [15] Yuri A. Kuznetsov, *Elements of Applied Bifurcation Theory* (Springer-Verlag, New York, 2010).
- [16] O. Galor, *Discrete Dynamical Systems* (Springer, New York 2010).
- [17] E. E. Sel'kov, Eur. J. Biochem. **4** 79 (1968).
- [18] I. Lengyel, G. Rabai, and I. R. Epstein, J. Am. Chem. Soc, **112** 9104 (1990).
- [19] I. Lengyel and I. R. Epstein, Science, **251** 650 (1991).

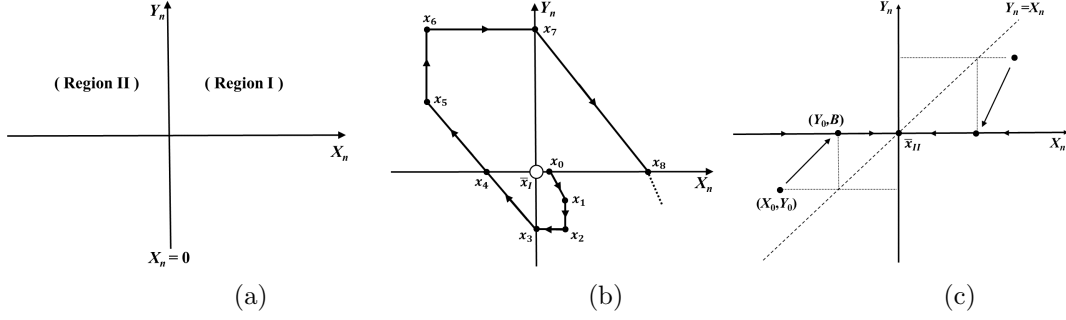


Figure 1: (a) Definition of regions I and II. (b) A trajectory in the vicinity of the unstable focus \bar{x}_I . (c) Trajectories obtained from Eq. (5).

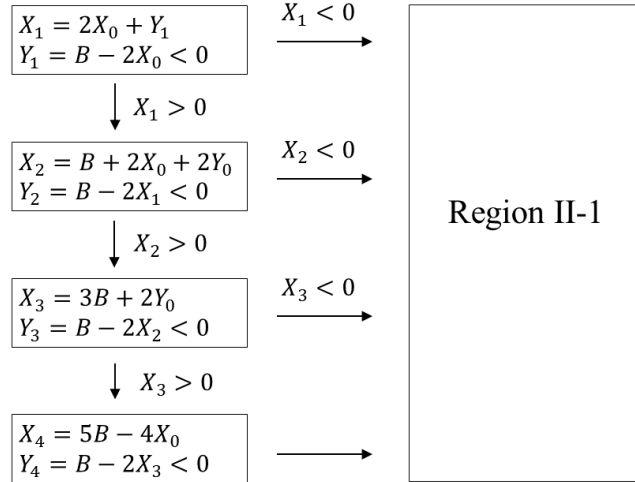


Figure 2: Flowchart for time evolutions of \mathbf{x}_n from the initial state (X_0, Y_0) in region I. (X_0, Y_0) moves into region II-1 within four iteration steps.

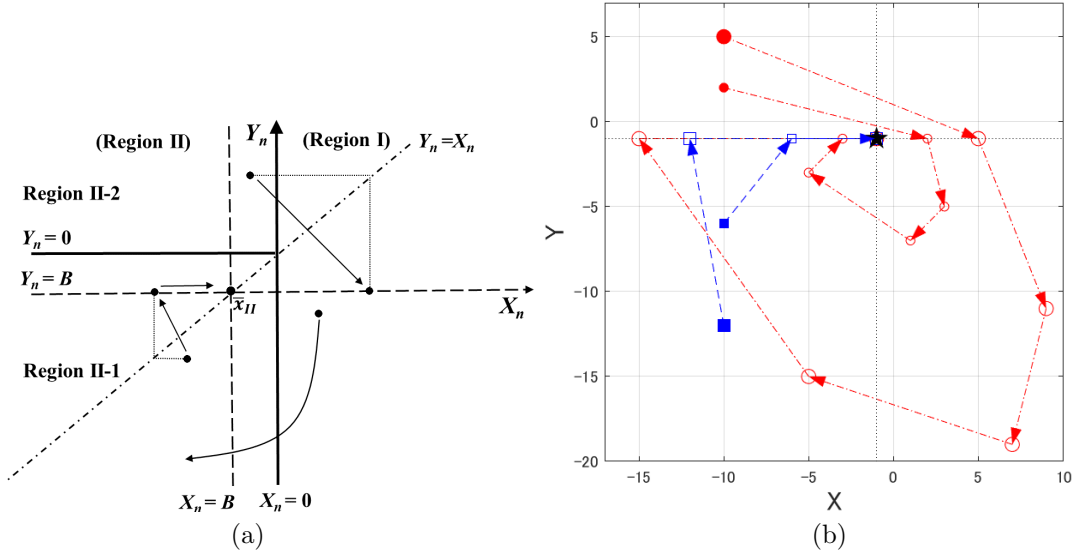


Figure 3: Trajectories obtained from Eqs. (1)-(2) with $B \leq 0$. (a) Schematic explanation. (b) Numerical results from four different initial states described by filled circles and squares. Trajectories proceed in the direction of the arrows and finally reach the stable fixed point \bar{x}_{II} shown by the black star.

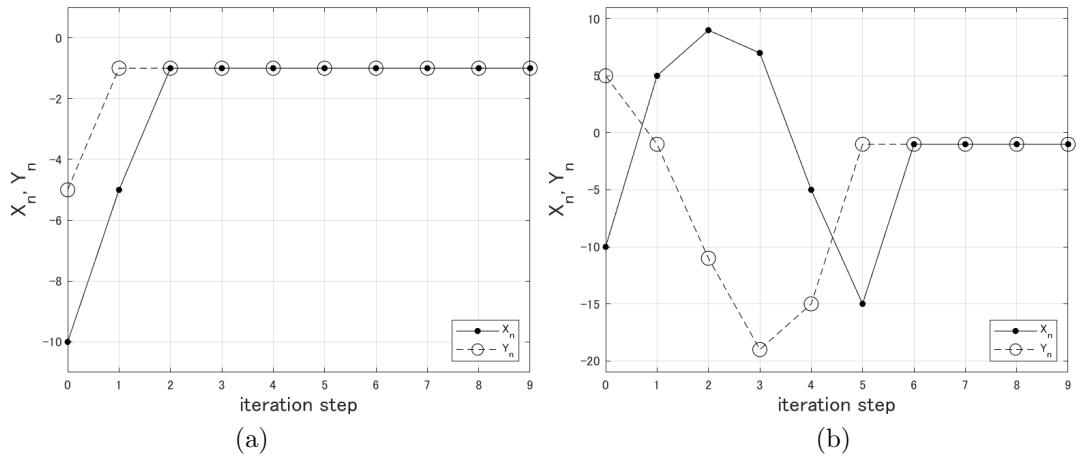


Figure 4: (X_n, Y_n) as a function of n for Eqs. (1)-(2) with $B = -1$ from two different initial conditions.

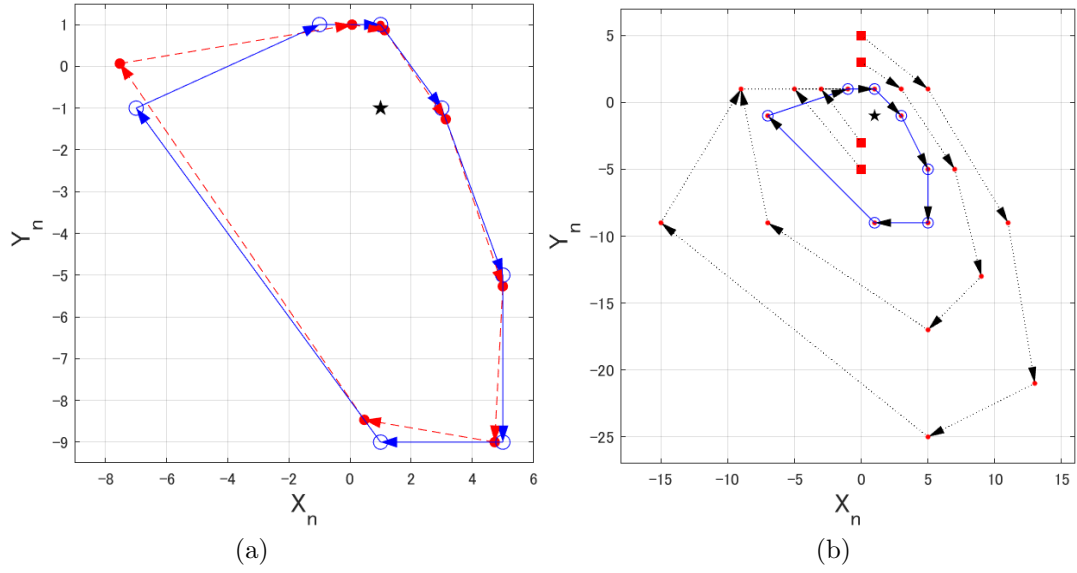


Figure 5: (a) The two limit cycles \mathcal{C} (open circles) and \mathcal{C}_s (filled circles). (b) Examples of trajectories starting from four different filled squares. The trajectories finally converge into \mathcal{C} . The star in each figure shows \bar{x}_I .